

Mitochondrial Genome and Nuclear Sequence Data Support Myzostomida As Part of the Annelid Radiation

Christoph Bleidorn,* Igor Eeckhaut,† Lars Podsiadlowski,‡ Nancy Schult,§ Damhnait McHugh,§ Kenneth M. Halanych,|| Michel C. Milinkovitch,¶ and Ralph Tiedemann*

*Unit of Evolutionary Biology/Systematic Zoology, Institute of Biochemistry and Biology, University of Potsdam, Potsdam-Golm, Germany; †Marine Biology Laboratory, University of Mons-Hainaut, Av. Champs de Mars 6, B-7000 Mons, Belgium; ‡Animal Systematics and Evolution, Institute for Biology, Zoology, Free University Berlin, Berlin, Germany; §Department of Biology, Colgate University; ||Department of Biological Sciences, Auburn University; and ¶Free University of Brussels, Institute of Molecular Biology and Medicine, Laboratory of Evolutionary Genetics, Gosselies, Belgium

The echinoderm symbionts Myzostomida are marine worms that show an enigmatic lophotrochozoan body plan. Historically, their phylogenetic origins were obscured due to disagreement about which morphological features are evolutionarily conserved, but now most morphological evidence points to annelid origins. In contrast, recent phylogenetic analyses using different molecular markers produced variable results regarding the position of myzostomids, but all suggested these worms are not derived annelids. To reexamine this issue, we analyzed data from nuclear genes (18S rDNA, 28S rDNA, Myosin II, and Elongation Factor-1 α), and a nearly complete myzostomid mitochondrial genome. Here, we show that the molecular data are in agreement with the morphological evidence that myzostomids are part of the annelid radiation. This result is robustly supported by mitochondrial (gene order and sequence data) and nuclear data, as well as by recent ultrastructural investigations. Using Bayes factor comparison, alternative hypotheses are shown to lack support. Thus, myzostomids probably evolved from a segmented ancestor and gained a derived anatomy during their long evolutionary history as echinoderm symbionts.

Introduction

Myzostomida are flat-bodied marine worms (fig. 1A) comprising about 170 species in 12 genera and the monophyly of the whole group is well supported (Lanterbecq et al. 2006). Myzostomids are usually ectocommensals or parasites of echinoderms (Grygier 2000; Eeckhaut and Lanterbecq 2005), and their association with echinoderms is presumably very old, with parasitized crinoid fossils dating back to the Carboniferous (~300–360 mya), and some pits attributed to myzostomids being found on crinoid fossils from the Ordovician (~444–488 mya) (Eeckhaut 1998). This long history as host-specific symbionts explains the highly modified myzostomid anatomy (fig. 1) and has obscured their phylogenetic position within Lophotrochozoa.

Phylogenetic affinities of the enigmatic Myzostomida have been the source of 2 centuries of dispute among systematists. Originally described as trematode flatworms (Leuckart 1827), Myzostomida were subsequently designated as Crustacea (Semper 1858), and later grouped together with pentastomids and tardigrades in Stelechopoda by Graff (1877). However, at the end of the 19th and the beginning of the 20th centuries, many researchers agreed that myzostomids are closely related to annelids (Benham 1896; Fedotov 1929; Kato 1952). Both myzostomid and annelids possess parapodia-like structures (fig. 1B) (Jägersten 1936), chitinous chaetae (fig. 1C) (Jägersten 1936), a ladder-like nervous system (Müller and Westheide 2000), and a trochophore-like larva (fig. 1D) (Eeckhaut, Fievez, and Müller 2003); they also both display serial nephridia, which suggests that they evolved from a segmented ancestor (Pietsch and Westheide 1987). On the other hand, myzostomids possess many unique characteristics such as

(1) unique organs thought to be sensory in function, i.e., the lateral organs (Eeckhaut and Jangoux 1993), (2) cyst-cells associated with developing male gametes and unique genital systems (Eeckhaut and Jangoux 1991; Eeckhaut and Lanterbecq 2005), and (3) a nutrient-deriving system relying on digestive diverticula and not on a coelomic or a vascular system (Eeckhaut, Dochy, and Jangoux 1995). Even the parapodial-like structures of myzostomids are highly specialized (Lanterbecq et al. submitted), making their homology with annelid parapodia suspect. Unlike larger annelids, their body cavity is filled with parenchymal cells, and a coelom is apparently lacking (see Eeckhaut and Lanterbecq 2005). Note, however, that some small annelids are also acoelomate (Smith, Lombardi, and Rieger 1986; Rouse and Pleijel 2001).

The annelid affinity of myzostomids has been challenged in recent times by morphological (Haszprunar 1996), molecular (Eeckhaut et al. 2000; Littlewood et al. 2001; Giribet et al. 2004; Passamanek and Halanych 2006), and combined analyses (Zrzavy, Hypsa, and Tietz 2001). Haszprunar's (1996) morphological cladistic analysis placed myzostomids with a sipunculid + echiurid + annelid clade. Given that echiurids and sipunculids appear to be within the annelid radiation (McHugh 1997; Boore and Staton 2002; Bleidorn, Vogt, and Bartolomaeus 2003; Jennings and Halanych 2005; Bleidorn, Podsiadlowski, and Bartolomaeus 2006), these morphological cladistic results seem to reflect the view based on traditional interpretations of morphological features grouping myzostomids with annelids and allied taxa (Echiura, Sipunculida).

Of the molecular and combined analyses mentioned above, only those of Eeckhaut et al. (2000) and Zrzavy, Hypsa, and Tietz (2001) were specifically designed to examine the placement of myzostomids; the others have only included a single myzostomid representative to address other issues of bilaterian relationships. Interestingly, in all of these studies myzostomids fall outside the annelid radiation. Eeckhaut et al. (2000) used 18S and EF-1 α and placed myzostomids with flatworms (with strong bootstrap

Key words: Myzostomida, Annelida, Myosin II, mitochondrial genome, gene order, long branch attraction.

E-mail: Bleidorn@uni-potsdam.de.

Mol. Biol. Evol. 24(8):1690–1701. 2007

doi:10.1093/molbev/msm086

Advance Access publication May 4, 2007

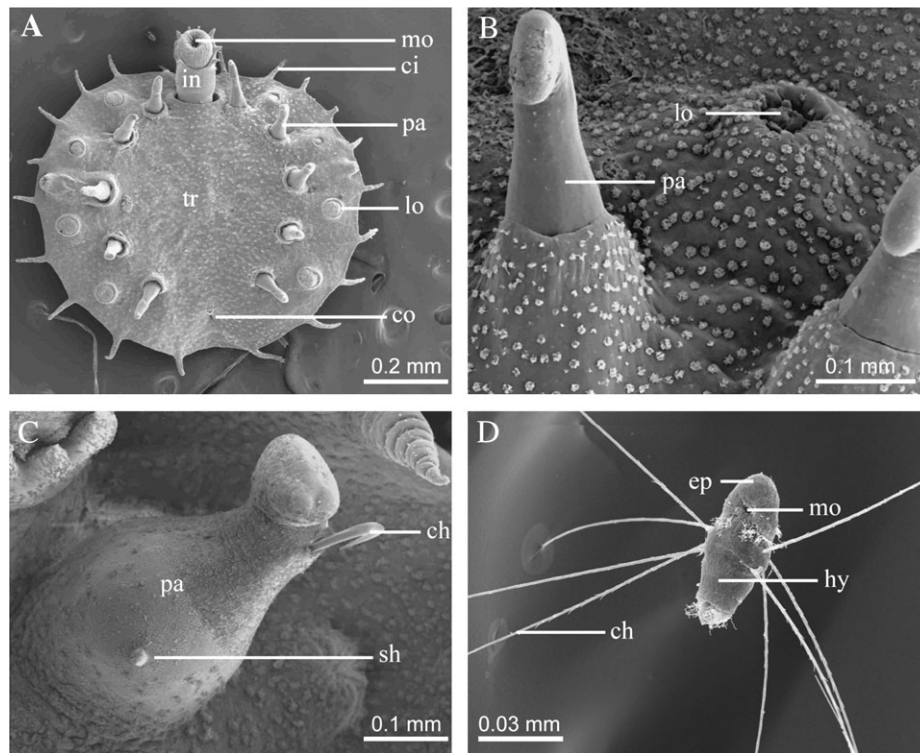


FIG. 1.—SEM views of some myzostomid features. Ventral side of *Myzostoma cirriferum* showing the iteration of external structures (A). A classical myzostomid parapodium and lateral organ (B). A type of parapodium that exists in about 20 species of myzostomids where the base bears a small hump that may be homologous to the neuropodial cirrus of polychaetes (C). myzostomid metatrochophore of *M. cirriferum* (D). ch = chaeta; ci = cirrus; co = cloacal opening; ep = episphere; hy = hyposphere; in = introvert; lo = lateral organ; mo = mouth; pa = parapodium; sh: small hump; tr = trunk.

support). Furthermore, they employed simulations to rule out the possibility that myzostomids were grouped to flatworms due to the “long-branch attraction” phenomenon (Felsenstein 1978). A few months later, Zrzavy, Hypsa, and Tietz’s (2001) analysis of 18S and morphology placed myzostomids in a new taxon called Promastigozoa uniting myzostomids with Syndermata (rotifers and acanthocephalans)—a clade that was mainly supported by spermatozoan ultrastructural characters (see also Mattei and Marchand 1987). This result was somewhat congruent with Eeckhaut et al. (2000), although the latter study did not include Syndermata. Finally, in a recent analysis using 18S rDNA as well as a complete 28S rDNA sequence of *Myzostoma polycyclus*, Passamaneck and Halanych (2006) placed myzostomids within bryozoans. Although supported by a high bootstrap value (84%), the authors suspected that this relationship was an artefact due to long-branch attraction.

A reliable resolution of the phylogenetic position of myzostomids is crucial for a better understanding of character evolution within Lophotrochozoa. If we accept that myzostomids are not closely related to annelids, as suggested by all previous molecular studies, then we have to assume that similarities present in these taxa are due to convergences or represent plesiomorphic traits. Alternatively, if myzostomids are highly derived annelids, character mapping of myzostomid body features will improve our understanding of the long-term consequences of parasitism and ectocommensalism. In an attempt to robustly resolve the phylogenetic position of myzostomids, we extended

the available molecular data set and examined 4 nuclear genes (18S rDNA, 28S rDNA, myosin II, and EF-1 α) as well as a large proportion of a myzostomid mitochondrial genome from *Myzostoma seymourcollegiorum*, (including 10 protein-coding genes, 2 ribosomal genes, and 14 tRNAs). We focused on testing the hypothesis of a monophyletic Myzostomida-Annelida grouping, so that the uncertainty regarding myzostomid evolutionary relationships can be settled.

Material and Methods

Data Collection

Six different datasets were compiled: 18S rDNA, 28S rDNA, EF-1 α , Myosin II, mitochondrial genome sequence data, and mitochondrial gene order. Sequence data of other protostomes and outgroup taxa (Echinodermata + Enteropneusta) were downloaded from GenBank (see supplementary table 1–4 for lists of taxa included in the different datasets and GenBank accession numbers).

DNA extraction was performed using the Qiagen DNeasy Tissue Kit (Qiagen, Germany) according to the manufacturer’s instructions. Samples for RNA extraction were collected and preserved in RNAlater (Invitrogen) or frozen at -80°C . Total RNA was isolated using RNAwizTM (Ambion) and reverse transcribed to cDNA using SuperScript II (Invitrogen).

We generated additional nuclear ribosomal gene sequences (28S rDNA) from *Myzostoma cirriferum* (collected

Table 1
PCR Primer Sequences and Annealing Temperatures Used for Long-Range PCR of mtDNA from *M. seymourcollegiorum*

Name	Sequence	Ann. Temp.
Myse-col1f(-cybr)	ATTTTATTATTATTATCATTACCAGTTTTAGC	54°C
Myse-cybr(-col1f)	TAGAAGAATAGTATGGGTGAAAAGG	54°C
Myse-cybf(-nd4r)	CCTTTTCACCCATACTATTCTTC	51°C
Myse-nd4r(-cybf)	AGTGGTAACCTAGCAATTACAGTG	51°C
Myse-nd4f(-12Sr)	TTTAAATCAAATTATAGTAAACTCGAAC	52°C
Myse-12Sr(-nd4f)	ATTATATTTATCACCGCCATTCTC	52°C
Myse-12Sf(-16Sr)	TCAGCTTGTGCATTGCCG	54°C
Myse-16Sr(-12Sf)	TGTTTTCCTTCATACAATCTCTCC	54°C

from its crinoid host *Antedon bifida* in Morgat, France) and *Myzostoma seymourcollegiorum* (kindly provided by G.W. Rouse, see Rouse and Grygier (2005) for a description of the collection site in Southern Australia). Ribosomal genes were amplified using primers and conditions as specified in Bleidorn (2005) for the complete 18S rRNA gene and as in Passamanek and Halanych (2006) for the complete 28S rRNA gene. Products were sequenced with an ABI Prism 3100 Genetic Analyzer and Big Dye Terminator v.3.1 (Applied Biosystems).

A fragment of the coding region of the Myosin II gene was sequenced from *Pulvinomyzostomum pulvinar*, *Myzostoma alatum*, and *Myzostoma cirriferum* (specimens as described in Eeckhaut et al. 2000). Amplification of Myosin II was carried out using nested degenerate primers (mio3 and mio4 designed by Ruiz-Trillo et al. (2002); and Mio-F: 5'-TCTTCAACCAACATGTTTCG-3' and Mio-R 5'-TTGGGRATRATRCADCKSAC-3'), with the external and internal pairs being mio3/mio4 and Mio-F/Mio-R, respectively. An initial touchdown PCR was performed (from 60°C to 55°C decreasing 1°C per 3 cycles, then from 55°C to 45°C decreasing 0.5°C per cycle for 21 cycles followed by 20 cycles at 45°C), and the products were reamplified at 50°C for 35 cycles. The TOPO TA Cloning Kit for Sequencing (Invitrogen) was used to clone the MyoII products (~565 bp), which were then bidirectionally sequenced with an ABI Prism 310 Genetic Analyzer and Big Dye Terminator v.3.1 (Applied Biosystems) using the standard T3/T7 primers.

A contiguous ~12kb fragment of the mitochondrial genome was determined from *Myzostoma seymourcollegiorum*. To generate mitochondrial genome data, small fragments of the *rrnL*, *cox1*, *cob*, and *nad4* genes were amplified using conserved primers as described in Bleidorn, Podsiadlowski, and Bartolomaeus (2006) and the *rrnS* gene with the primer pair described in Podsiadlowski and Bartolomaeus (2005). All products were purified with the BlueMatrix DNA purification kit (EURx). Sequencing reactions were performed with a dye terminator procedure and run on a CEQ 8000 (Beckman Coulter) or on an ABI Prism 3100 (Applied Biosystems) according to the recommendations of the manufacturer. In a second step, the determined sequences were used to design 4 additional PCR primer pairs (table 1) bridging the gaps between *rrnS-rrnL*, *cox1-cob*, *cob-nad4*, and *nad4-rrnS*. A long-PCR approach using these primer pairs was performed using Takara LA-Taq (MoBiTech). The 50- μ l reaction volumes were set up as follows: 29.5 μ l sterilized distilled water, 5 μ l 10 \times reaction buffer, 5 μ l MgCl₂-solution, 8 μ l dNTP mix, 1 μ l

primer mix (10 μ M each), 1 μ l DNA template, 0.5 μ l (1u) Takara LA-Taq polymerase. A touchdown PCR approach was used for these fragments: 94°C for 3 min; 7 cycles with 94°C for 1 min, 63°C for 1 min (-0.5°C in every step), and 70°C for 8 min; 35 cycles with 94°C for 1 min, 60°C for 1 min 30 s, and 70°C for 8 min; final extension at 70°C for 10 min. PCR purification of these fragments was done using BlueMatrix DNA purification kit (EURx). The fragment spanning between *cox1* and *cob* was cloned into pGEM T-easy vector (Promega) and sequenced initially using vector primers M13f/r and further on by primer walking. The 3 other fragments were sequenced directly from PCR products with PCR primers, then internally by primer walking.

Protein-coding genes and ribosomal RNA genes were identified by blasting on NCBI Entrez databases and by comparing with other mitochondrial genomes using DOGMA (Wyman, Jansen, and Boore 2004). Boundaries of ribosomal genes could not be identified by sequence homology alone and were inferred from the boundaries of flanking genes. Transfer RNA genes were identified by their potential secondary structures using the tRNAscan-SE Search Server (Lowe and Eddy 1997). Transfer-RNA identity was specified by its anticodon sequence.

Alignment

Metazoan ribosomal sequences, including their suggested alignment based on secondary structure, were downloaded already aligned from the ribosomal database project II (<http://rdp8.cme.msu.edu/html/>). Other ribosomal sequences taken from GenBank were aligned, together with our new sequences, to the previously assembled ribosomal sequences using Clustal X (Jeanmougin et al. 1998) with the profile alignment option. We used the program GBLOCKS v. 0.91b (Castresana 2000) to exclude unreliably aligned positions. For EF-1 α and Myosin II, sequences were translated into amino acids, aligned with Clustal W (Thompson, Higgins, and Gibson 1994) as implemented in Bioedit (Hall 1999), and back translated to nucleic acids. DAMBE (Xia and Xie 2001) was used to check for saturation of each codon position of protein coding nucleotide datasets; only the third codon position was saturated and consequently excluded.

Amino acid sequences of protein coding genes present in the sequenced fragment of the mitochondrial genome of *Myzostoma seymourcollegiorum* (*atp6*, *cox1*, *cox2*, *cox3*,

cytb, *nad4*, *nad4L*, *nad5*, *nad6*) were aligned with GenBank sequences using Clustal W (Thompson, Higgins, and Gibson 1994) as implemented in Bioedit (Hall 1999); *atp8* was excluded because it is not present in Platyhelminthes or Syndermata. The program GBlocks v. 0.91b (Castresana 2000) was used to exclude regions of ambiguous alignment. Mitochondrial gene order data was aligned using CIRCAL (Fritsch, Schlegel, and Stadler 2006). The alignment was translated into a nexus-style absence/presence matrix for subsequent phylogenetic analysis. All alignments were deposited in Treebase (www.treebase.org).

Phylogenetic Analysis

Stationarity of nucleotide frequencies was estimated for all nucleotide datasets using a χ^2 test under the base frequencies option in PAUP*4b10 (Swofford 2002). Deuterostome taxa (Enteropneusta and Echinodermata) served to root the trees of all analyses.

Mitochondrial Data

The absence/presence matrix of mitochondrial gene order data was analyzed with Maximum Parsimony under the branch-and-bound search option in PAUP* 4b10 (Swofford 2002). Node support was estimated from 1,000 bootstrap replicates under TBR branch-swapping.

For the mitochondrial genome sequences, we partitioned the data into 9 character sets, each containing the amino acid data of 1 of the 9 protein coding genes (*cox1-3*, *cob*, *nad4-6*, *atp6*). Models were selected for each single partition as well as for the concatenated dataset of all protein coding genes using the AIC as implemented in ProtTest 1.3 (Abascal, Zardoya, and Posada 2005).

Maximum Likelihood (ML) analysis was conducted under the model selected for the concatenated dataset using PHYML (Guindon and Gascuel 2003) with 4 rate categories, gamma shape and number of invariant sites estimated from the data. Clade stability was estimated by 500 replicates of nonparametric bootstrapping.

For Bayesian analysis using MrBayes 3.1.2 (Ronquist and Huelsenbeck 2003), the amino-acid substitution model was set independently for each partition according to the results of the ProtTest analyses (see table 2) and all parameters were unlinked. Two independent runs, each with 4 Markov chains, were run in parallel (starting each from a random tree) for 1,000,000 generations, with trees being sampled every 250 generations for a total of 4,001 trees. An average standard deviation of split frequencies <5% was used as the indication for convergence. After convergence of likelihood, the first 1,230 trees were discarded as *burn in*, and posterior probabilities were estimated as the frequency of clades in the 2,771 sampled trees.

Myosin II, EF-1 α , and 18S

Nucleotide substitution models were selected for all data sets using the Akaike Information Criterion (AIC) implemented in Modeltest 3.07 (Posada and Crandall 1998). ML analyses were conducted using PHYML (Guindon and

Table 2
Properties of Single Gene Partitions of the Concatenated Mitochondrial Protein Data Set

Gene	Positions in Full Alignment	Positions Finally Used in Analyses	Chosen Model Using AIC in Prottest
<i>atp6</i>	290	53	MtREV + G
<i>cox1</i>	643	486	MtREV + I + G
<i>cox2</i>	242	183	Blosum62 + I + G
<i>cox3</i>	270	180	MtREV + G
<i>cob</i>	389	313	MtREV + G
<i>nad4</i>	476	229	MtREV + I + G
<i>nad4L</i>	105	18	MtREV + G
<i>nad5</i>	657	265	MtREV + I + G
<i>nad6</i>	189	13	MtREV
combined data set	3261	1740	MtREV + I + G

Gascuel 2003) with 4 rate categories; gamma shape and number of invariant sites were estimated from the datasets. Clade stability was estimated by nonparametric bootstrapping in 500 replicates for all datasets.

Bayesian analyses were conducted using MrBayes 3.1.2 (Ronquist and Huelsenbeck 2003). Nucleotide models were set according to the results obtained with Modeltest. Two independent runs, each with 4 Markov chains, were run in parallel (starting each from a random tree) for 500,000 generations (in the case of EF-1 α and Myosin II) or 30,000,000 generations (18S), with trees being sampled every 500 generations. An average standard deviation of split frequencies <5% was used as the indication for convergence. After convergence of likelihood, trees were discarded as *burn in*, and posterior probabilities were estimated as the frequency of clades in the trees sampled after standard deviation of split frequencies fell below 5%.

28S

Analysis of our 28S dataset indicates significant ($P < 0.001$) nonstationarity of nucleotide frequencies among lineages, a bias that can cause systematic errors in phylogeny reconstruction (Simon et al. 2006). Jermini et al. (2004) have shown that Maximum Parsimony (MP) and Maximum Likelihood (ML) methods have difficulties inferring the correct tree in simulated datasets with compositional heterogeneity and short internal edges—the latter instance is observed in most ribosomal datasets inferring deep metazoan phylogeny. Methods using LogDet distances (Steel 1994) perform better under compositional heterogeneity (e.g., Jermini et al. 2004). Therefore we used the Minimum Evolution (ME hereafter) criterion with trb-branch swapping using LogDet-data transformations as implemented in PAUP* for phylogenetic inference of the 28S dataset. Clade support was assessed by nonparametric bootstrapping in 500 replicates. We also used Tree-Puzzle 5.0 (Schmidt et al. 2002) to identify which sequences fail a 5% test of base compositional heterogeneity. If we omitted all taxa which failed the test, we would exclude syndermatans (a taxon which is clustering with myzostomids in Zrzavy, Hypsa, and Tietz 2001), *Dugesia* (the flatworm which clustered with myzostomids in Eeckhaut et al.

2000), as well as those bryozoans (*Crisia* and *Bugula*) clustering together with myzostomids in Passamaneck and Halanych (2006). An analysis with such a limited taxonomic sampling would be unable to discriminate among the hypotheses of interest.

Investigating Long-Branch Attraction

The position of Myzostomida in previous phylogenetic analyses of nuclear ribosomal gene data was suspected to be a possible artifact of long-branch attraction (LBA) (Passamaneck and Halanych 2006). Recently, Kennedy et al. (2005) have shown that methods such as spectral analysis can be used to detect conflicting signals within the data, including those caused by LBA. Therefore, we performed a spectral analysis of both ribosomal datasets using the program PHYSID (Wägele and Rödding 1998) as implemented in the SAMS package (Mayer and Wägele 2005). In spectral analyses, support for a split depends on the number of characters in the alignment whose pattern corresponds to that split (Kennedy et al. 2005). We limited noise to 25% of the positions of a single row of supporting positions. We visualized the spectrum of the 30 best splits sorted by the total number of supporting positions.

Furthermore, we performed parametric simulation studies (Huelsenbeck 1997) to investigate whether the branches of myzostomids and bryozoans (or other nonannelid long branched taxa) in the 28S dataset are long enough to attract, even though they are not each others closest relatives. The best-fitting model for the original dataset was estimated with Modeltest, and we analyzed the data with annelid + myzostomid monophyly constrained with ML using the model parameters. We used this model tree and model parameters to simulate 100 replicated data sets with Seq-Gen v. 1.3.2 (Rambaut and Grassly 1997). The replicated datasets were analyzed with ME (under LogDet-data transformations as in the original analysis), equally weighted MP, and ML using the estimated model parameters. For comparison, the original dataset was also analyzed by MP and ML with the settings described above. All analyses were conducted with PAUP*4b10.

Bayes Factor Comparison

For hypothesis testing in the Bayesian framework, we used the Bayes factor (Kass and Raftery 1995; Nylander et al. 2004). Harmonic means of the likelihood values of the Markov chain Monte Carlo samples of the Myosin II and mitochondrial protein data set were calculated with MrBayes as described above. We then calculated the harmonic mean of the likelihood values of alternative hypotheses. In these cases, tree topologies were constrained to contain monophyletic Myzostomida + Platyhelminthes, Myzostomida + Syndermata, or Myzostomida + Bryozoa (only for the mitochondrial data set) for the same sample of trees. Twice the difference in log likelihoods can be used to estimate the extent to which the observed result (unconstrained tree) differed from the null hypothesis (constrained trees). Values >10 are considered to be very strong support for the alternative hypothesis (Nylander et al. 2004), which is the unconstrained tree in this setting.

Results

Mitochondrial Data

Gene order in the mitochondrial genome of *Myzostoma seymourcollegiorum* revealed several striking similarities with known annelid genomes (fig. 2). The order of protein coding genes of *M. seymourcollegiorum* is identical compared to that of annelids (except the echiurid *Urechis*). Furthermore, 2 sets of adjacent genes in conserved order can be found within all hitherto investigated annelids and the myzostomid: (1) *trnQ*, *nad6*, *cob*, *trnW*, *atp6*, *trnR*; (2) *trnT*, *nad4L*, *nad4*. Finally, all genes are transcribed from the same strand in myzostomids and annelids. No common pattern can be found when comparing the gene order of Myzostomida with that of Bryozoa, Syndermata, or different Platyhelminthes (see fig. 2 for comparison with platyhelminth taxa which have not been included in the subsequent phylogenetic analysis). A phylogenetic analysis of aligned gene order data across protostomes recovers an Annelida + Myzostomida clade (fig. 3A), which is strongly supported through parsimony bootstrapping (92%).

The concatenated mitochondrial protein dataset consisted of 1,740 unambiguously aligned amino acids (see table 2 for contribution of each gene). The dataset was analyzed both with the mtREV + I + Γ model and under a mixed model setting, i.e., with each partition being assigned the best substitution model suggested by ProtTest (table 2). MrBayes analyses (fig. 3B) as well as ML analyses (fig. 1 in supplementary data) recover an annelid + myzostomid clade that is significantly supported by posterior probabilities (1.0), but not through ML-bootstrapping. The monophyly of Brachiopoda and Platyhelminthes is recovered and well supported by both analyses; molluscs appear paraphyletic.

A Bayes factor comparison favors the best tree (including the Annelida + Myzostomida clade) when compared with hypotheses where myzostomids are constrained to group with Bryozoa (twice the difference of total harmonic mean ln likelihood is 55.32), Platyhelminthes (169.94), or Syndermata (76.9).

Myosin II

After excluding third codon positions, the Myosin II-dataset consists of 436 nucleotide sites. Base frequencies do not significantly deviate from stationarity. GTR + I + Γ was selected as the best-fitting model. The inclusion of myzostomids within annelids (fig. 3C) is supported by ML bootstrapping (96%), as well as by Bayesian posterior probabilities (1.0). Mollusca and Platyhelminthes are recovered as monophyletic groups.

A Bayes factor comparison strongly supports the best tree (including the annelid + myzostomid clade), when compared with trees, where myzostomids are constrained to group with Platyhelminthes (66.2) or Syndermata (49.4). Unfortunately, there are no Myosin II data for Bryozoa available.

EF-1 α

After excluding third codon positions, the EF-1 α -dataset consists of 716 nucleotide sites. Base frequencies do not

Lumbricus, *Helobdella* (part), *Riftia* (part), *Galathealinum* (part) and *Clymenella* (with the exception that K is between nc and H)

cox1	N	cox2	D	atp8	Y	G	cox3	Q	nad6	cob	W	atp6	R	nc	H	nad5	F	E	P	T	nad4L	nad4	C	M	rrnS	V	rrnL	L1	A	S2	L2	nad1	I	K	nad3	S1	nad2
------	---	------	---	------	---	---	------	---	------	-----	---	------	---	----	---	------	---	---	---	---	-------	------	---	---	------	---	------	----	---	----	----	------	---	---	------	----	------

Orbinia (Annelida)

cox1	N	cox2	D	atp8	Y	cox3	Q	nad6	cob	W	atp6	R	A	H	nad5	F	E	P	T	nad4L	nad4	C	L2	nc	L1	M	rrnS	V	rrnL	S2	nad1	I	K	nad3	S1	nad2	G
------	---	------	---	------	---	------	---	------	-----	---	------	---	---	---	------	---	---	---	---	-------	------	---	----	----	----	---	------	---	------	----	------	---	---	------	----	------	---

Urechis (Echiura, Annelida)

cox1	cox2	P	D	atp8	T	nad4L	nad4	M	N	G	nad2	Y	L1	A	S2	L2	nad1	I	K	nad3	rrnS	rrnL	V	S1	cox3	nc	Q	nad6	cob	W	atp6	R	H	nad5	F	C	E
------	------	---	---	------	---	-------	------	---	---	---	------	---	----	---	----	----	------	---	---	------	------	------	---	----	------	----	---	------	-----	---	------	---	---	------	---	---	---

Platynereis (Annelida)

cox1	N	cox2	G	nc	Y	atp8	M	D	cox3	Q	nad6	cob	W	atp6	R	H	nad5	F	E	P	T	nad4L	nad4	rrnS	V	rrnL	L1	S2	A	L2	nad1	I	K	nad3	S1	nad2	C
------	---	------	---	----	---	------	---	---	------	---	------	-----	---	------	---	---	------	---	---	---	---	-------	------	------	---	------	----	----	---	----	------	---	---	------	----	------	---

Myzostoma seymourcollegiorum (Myzostomida)

cox1	N	cox2	atp8	D	Y	cox3	Q	nad6	cob	W	atp6	R	nad5	P	L2	E	T	nad4L	nad4	V	G	H	L1	rrnS	rrnL
------	---	------	------	---	---	------	---	------	-----	---	------	---	------	---	----	---	---	-------	------	---	---	---	----	------	------

Paratomella (Acoela)

cox1	K	nad2	nad6	rrnL	G	atp6	V	atp8	cox2	nad1	S2	D	I	rrnS	E	M	S1	cox3	Y	cob
------	---	------	------	------	---	------	---	------	------	------	----	---	---	------	---	---	----	------	---	-----

Microstomum (Platyhelminthes, Rhabditophora)

nad2																			cob	nad5	A	Q	rrnS	S2	rrnL	I	cox3	K	F	L2	atp6
------	--	--	--	--	--	--	--	--	--	--	--	--	--	--	--	--	--	--	-----	------	---	---	------	----	------	---	------	---	---	----	------

FIG. 2.—Mitochondrial gene order of *Myzostoma seymourcollegiorum* compared with annelids, a rhabditophoran flatworm, and a member of the Acoela. Protein-coding genes and ribosomal RNA genes were identified by blasting on the NCBI Entrez databases and by comparing with other annelid mitochondrial genomes using DOGMA (Wyman, Jansen, and Boore 2004). Transfer RNA genes were identified by their potential secondary structures using the tRNAscan-SE Search Server (Lowe and Eddy 1997). Identical patterns between taxa are highlighted. Abbreviations are as follow: ATP synthase subunits (*atp6*, *atp8*) cytochrome oxidase subunits (*cox1-cox3*), apocytochrome b (*cob*), nicotinamide adenine dinucleotide ubiquinone oxidoreductase subunits (*nad1-nad6*), small and large ribosomal subunit (*rrnS*, *rrnL*). Transfer RNA genes are denominated by the corresponding amino acid (oneletter code).

significantly deviate from stationarity. GTR + I + Γ was selected as the best-fitting model. ML analyses (Fig. 3D) group Myzostomida with a nematode (bootstrap support below 50%), whereas Bayesian inference recovered a clade consisting of molluscs and myzostomids, but without significant support (fig. 2 in the supplementary information). Neither annelids (*Capitella* is found outside all other annelids), nor Platyhelminthes (*Stylochus* is outside), nor Mollusca are recovered as monophyletic groups; *Dugesia* does not group with the other tricladid flatworms (*Crenobia*, *Girardia*, and *Schmidtea*). Most recovered clades lack bootstrap support (even myzostomid monophyly is supported by only 57% of the replicates).

Ribosomal Genes

After exclusion of ambiguous sites, the 28S and 18S datasets consist of 2,361 and 1,504 nucleotide sites. Stationarity of base frequencies was significantly rejected for the 28S dataset: 9 (of 35) taxa failed the 5% level χ^2 -test (see Materials and Methods). Taxa found to be significantly dif-

ferent include all outgroups (*Harrimania*, *Saccoglossus*, *Asterias*, and *Florometra*), both syndermatans (the rotiferan *Philodina* and the acanthocephalan *Oligocanthorhynchus*), 2 bryozoans (*Crisia* and *Bugula*), and a flatworm (*Dugesia*). No significant compositional heterogeneity was detected for the 18S dataset. GTR + I + Γ was selected as the best-fitting model for the 18S dataset, while the 28S was analyzed using a logdet-model (see above).

Whereas myzostomids group within Bryozoa in the ME analysis (fig. 4) of the 28S dataset (73% bootstrap support for a clade including all analyzed bryozoans and myzostomids), the position of myzostomids depends on the chosen method of analysis for the 18S dataset. Whereas ML recovers a *Symbion* + Myzostomida clade, Bayesian analyses supports a close relationship to some polychaete worms (figs. 3 and 4 in the supplementary information).

Investigating LBA

Spectral analyses show highly conflicting signals regarding the position of Myzostomida for both ribosomal

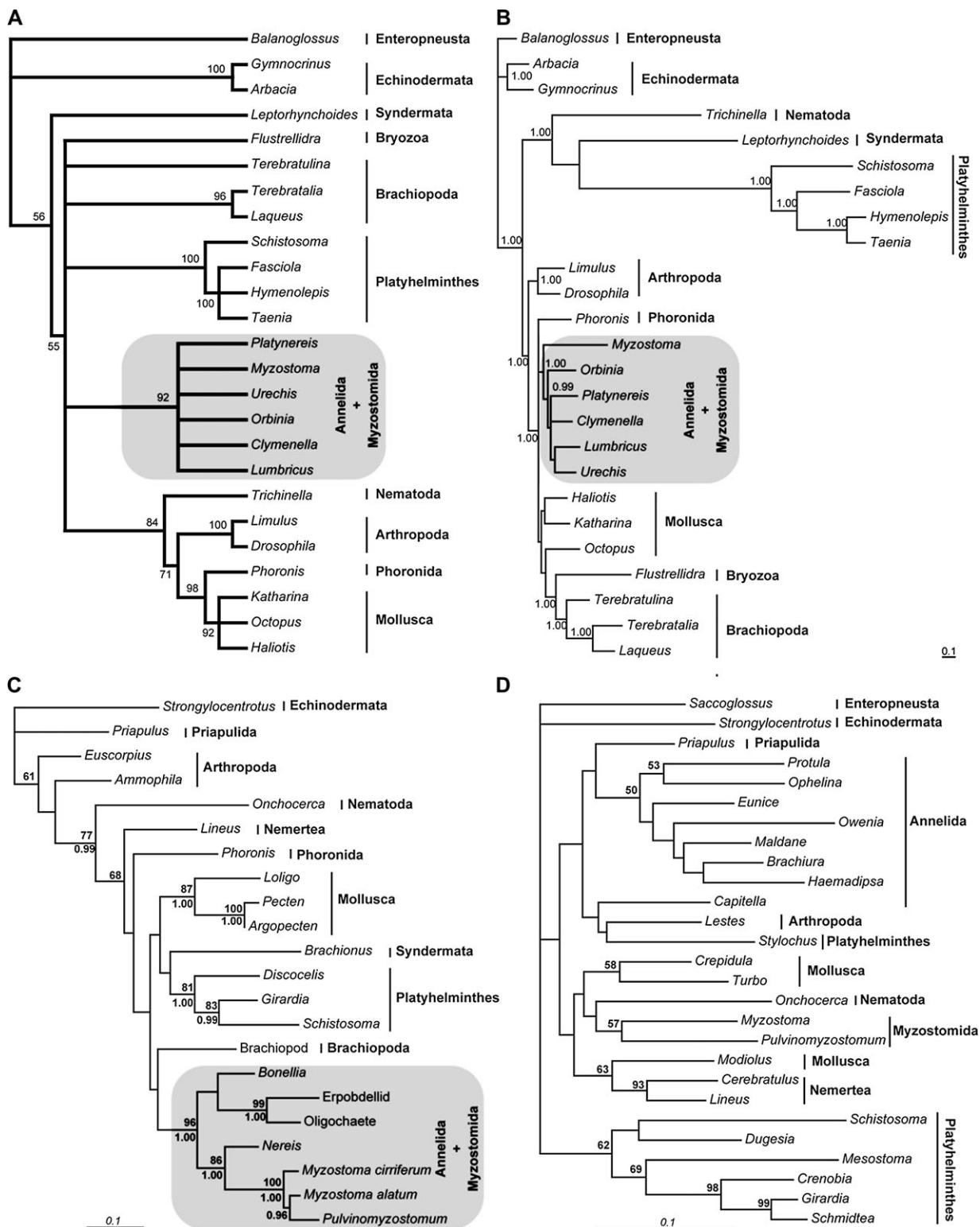


FIG. 3.—(A) Strict consensus tree of 76 equally parsimonious trees revealed by Maximum Parsimony analysis (using PAUP*4b10) of mitochondrial gene order data. Gene order data was aligned with CIRCAL (Fritzsch et al. 2006). Bootstrap support (1,000 replicates) is given at the nodes. Deuterostome taxa root the tree. (B) Bayesian analysis of the partitioned mitochondrial protein dataset, i.e., 1,749 amino acid positions concatenated from 9 mitochondrial protein sequences (*cox1-3*, *cob*, *atp6*, *nad4-nad6*). Analysis was conducted with MrBayes using, separately for each partition, the optimal model as inferred with ProtTest. Bayesian posterior probabilities are given at the nodes. Deuterostome taxa root the tree. (C) Maximum Likelihood analysis of the Myosin II dataset using PHYML with the GTR + I + Γ model. Bootstrap support estimated from 500 replicates is given below the branches. Posterior probabilities estimated with MrBayes using the same model are given below the branches. Deuterostome taxa root the tree. (D) Maximum Likelihood analysis of the elongation factor-1 α dataset using PHYML with the GTR + I + Γ model. Bootstrap support estimated from 500 replicates is given above the branches. Deuterostome taxa root the tree.

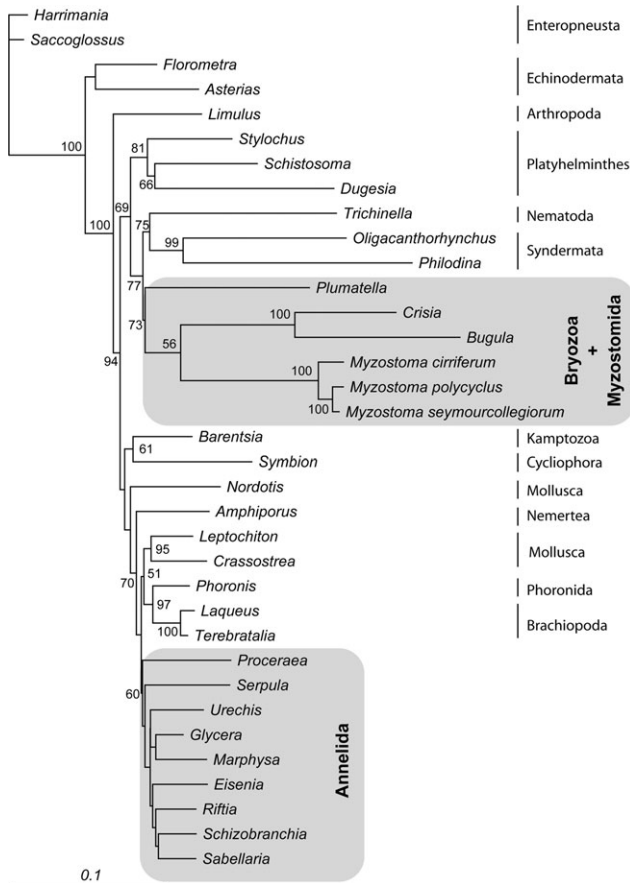


FIG. 4.—Minimum Evolution analysis of the 28S rDNA dataset using PAUP* 4b10 with LogDet distances. Bootstrap support estimated from 500 replicates is given above the branches. Deuterostome taxa root the tree.

genes. In the case of the 28S dataset, 13 splits grouping *Myzostoma* with other long-branched taxa can be found within the 30 best-supported splits (fig. 5), all of them standing in conflict to each other. Seventeen such splits are recovered within the 30 best-supported splits of the 18S dataset. This conflict points to potential artifacts in these phylogenetic analyses. Thus, in the case of myzostomids, the ribosomal sequences seem less reliable than other sources of data. The results of the simulation study of the 28S dataset are more inconclusive. MP and ML analyses of the original (unconstrained) dataset yielded trees congruent with that of the ME analysis. When analyzing the replicated datasets, ME never recovers the monophyletic annelid + myzostomid clade and always groups myzostomids with other long-branched taxa (*Trichinella*, Bryozoa), whereas MP recovers the correct clade only in 7% of all replicates. In contrast to this, ML always infers the correct clade. This means that the branches are long enough to artificially attract each other under ME and MP, but not when using the ML criterion with the correct model. However, we were not able to model unequal base-frequencies or even heterotachy in this study; both factors are likely to be present in the original analyses and are putatively misleading even the ML analysis.

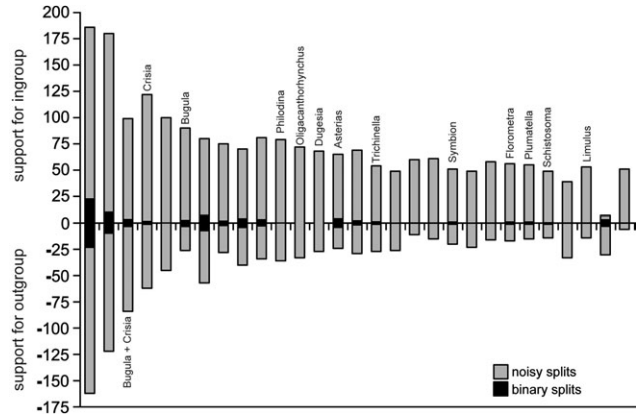


FIG. 5.—Spectrum for best 30 supported splits of the 28S dataset. Binary splits are shaded in black, noisy splits in grey. Splits are sorted by the total number of supporting positions (binary + noisy). Splits where myzostomids are grouped with other taxa are indicated by the name of those taxa. Analysis shows highly conflicting signals regarding the position of Myzostomida.

Discussion

Phylogenetic Position of Myzostomida

We present here evidence from mitochondrial and Myosin II data that Myzostomida have an annelid origin. The unique order of 10 protein-coding and 2 ribosomal genes shared by myzostomids and annelids, but not by any other metazoan taxon (see Vallés and Boore 2006 for a review of lophotrochozoan mitochondrial genomes), is compelling evidence supporting annelid affinities for Myzostomida. This gene order is also different from the hypothetical ground pattern of Bilateria (Lavrov and Lang 2005)—therefore gene order shared by annelids and myzostomids is unlikely to represent a plesiomorphic condition. While it is well known that tRNAs are more mobile than protein-coding mitochondrial genes (Boore 1999), in either case back-mutations restoring an ancestral genomic arrangement are highly unlikely. Therefore, there is little concern that homoplastic reversal events at the mitochondrial gene order level will obscure phylogenetic relationships (Boore and Brown 1998).

While our analyses of mitochondrial data recover myzostomids as sister to all annelids, they appear as derived within annelids in the case of the Myosin II data with strong support in all analyses. The usefulness of analyzing deep bilaterian phylogenies with this gene has been previously demonstrated by Ruiz-Trillo et al. (2002), who emphasized the homogenous rate of evolution as well as the homogeneity of nucleotide frequencies for all species studied. These properties are confirmed by our analyses, where myzostomids do not show significantly longer branches than all other included taxa.

The same suitable properties apply for the EF-1 α dataset. However, in agreement with previous analyses (Eeckhaut et al. 2000), myzostomids are placed outside annelids in analyses of this gene. In this case, the amount of phylogenetic information content for deep branching events seems to be too low, as most clades are only poorly supported through bootstrapping. In contrast to the analyses of Eeckhaut et al. (2000) and corroborating Littlewood

et al. (2001), our analyses of the EF-1 α dataset do not recover a clade uniting flatworms and myzostomids. It is likely that an erroneously high support for this hypothesis was an artifactual product of limited taxon sampling in the original analysis (besides myzostomids, annelids, and arthropods, only 1 flatworm and 1 mollusc were included). We conclude that the EF-1 α dataset does not significantly support any specific hypothesis regarding the phylogenetic position of myzostomids.

Our analyses of the nuclear ribosomal gene data confirm previous findings, at least partially; results of 18S analyses are ambiguous (ML groups myzostomids with Cycliophora, whereas Bayesian inference groups them with some polychaetes). However, in the case of the 28S dataset, myzostomids are placed outside annelids and instead cluster with bryozoans, a result previously found by Passamaneck and Halanych (2006). These authors suggested that this finding is likely influenced by long-branch attraction (LBA). It has been shown that LBA, the erroneous grouping of long branches, is not confined to any particular inference method (see Bergsten 2005 for a review on this issue). There is no direct way to detect LBA, but we would at least expect conflicting signal within a dataset as a potential indicator when assuming that the placement of a certain taxon is due to LBA. As Kennedy et al. (2005) have shown, methods such as spectral analysis are useful to detect conflicting signals within the data, including those causing LBA. Using this method, highly conflicting signal regarding the position of myzostomids was detected for both ribosomal gene datasets (18S and 28S). Parametric simulation studies conducted for the 28S data set additionally show that the branches of the bryozoans and myzostomids are long enough to attract each other in our ME-analysis. Combining this evidence, we conclude that the position of myzostomids (and other taxa) is likely to be influenced by LBA in our analyses of ribosomal genes.

Additionally, we did not find any support in favour of “Promastigozoa,” a taxon uniting myzostomids with syndermatans. The shortcoming of the morphological character matrix analyzed by Zrzavy, Hypsa, and Tietz (2001), which supports this clade, was extensively discussed previously (Jenner 2003).

We decided not to analyze a dataset combining all the molecular data presented here. Indeed, these datasets are not congruent in terms of taxon sampling, which means that we would have to combine different taxa in a single OTU, of which some are even not closely related, something we consider unwise and potentially misleading. We have shown that an annelid origin of Myzostomida is robustly supported by nuclear (Myosin II) and mitochondrial sequence data, as well as by genomic-level data, i.e., the mitochondrial gene order.

The sister group of Myzostomida remains unresolved, which is not surprising given that a robust phylogenetic hypothesis for annelids in general is lacking (Bartolomaeus, Purschke, and Hausen 2005; McHugh 2005). Much denser taxon sampling as well as additional molecular characters will be needed to robustly resolve the exact phylogenetic position of myzostomids within the annelid radiation. In a cladistic analysis of morphological data (Rouse and Fauchald 1997) including most known annelid families,

myzostomids were scored as segmented and grouped within the Phyllococida, a polychaete taxon with which they share the presence of Acicula (a special type of supportive chaetae also present in Eunicida, Amphinomida, and Orbiniidae), a specialized muscular proboscis, and the presence of metameric protonephridia in adult worms (found in at least some phyllococidans) (Rouse and Pleijel 2001; Bartolomaeus and Quast 2005). It will be interesting to test this hypothesis with additional genomic-level data and gene sequence data for a rich sampling of taxa within annelids.

Myzostomid Anatomy

The many unique features of Myzostomida have fuelled debates about the phylogenetic position of the group. A major point of contention has been whether Myzostomida are segmented animals and, if so, whether their segmentation is homologous with that of annelids (e.g., Haszprunar 1996; Zrzavy, Hypsa, and Tietz 2001). To further discuss this issue, we have first to clarify the definition of segmentation. Properties of segmentation have been intensively discussed elsewhere (e.g., Willmer 1990; Scholtz 2002; Seaver 2003; Tautz 2004). Usually a distinction is made between “true” segmentation and iteration (serial repetition). Whereas iteration includes all kinds of repetition of structures (Seaver 2003), segmentation is often linked to coelom formation (Willmer 1990; Seaver 2003; Tautz 2004). Scholtz (2002) defined true segmentation as repeated units along an anterior-posterior body axis, and each segment comprises a combination of structures with both ectodermal and mesodermal origins. Looking at myzostomids, we find that some structures are iterated, most obviously the parapodia-like structures (see fig. 1A). Pietsch and Westheide (1987) have shown that *Myzostoma cirriferum* also has serially arranged protonephridia, and a recent study revealed the metameric nature of the nervous system (Müller and Westheide 2000). However, all these structures are of ectodermal origin. The occurrence of a coelom—which is usually of mesodermal origin—in myzostomids is questionable. Recent ultrastructural investigation revealed that the female genital cavities of myzostomids, which are scattered in the parenchyma, are lined by an epithelium and thus represent secondary cavities (see Eeckhaut and Lanterbecq 2005); furthermore the ontogeny of these structures seems to be different from that of the annelid coelom, suggesting that it is not formed by bilateral mesodermal bands (unpublished data). Thus, there is no evidence for internally repeated coelomic cavities within myzostomids. Even the sequence of emergence of parapodia in juvenile myzostomids differs from a strict addition facilitated by a posterior growth zone. The parapodial structures appear in the following order during development: third pair, fourth pair, second and fifth pair (simultaneously), and first pair (Jägersten 1940). A recent developmental investigation of segmentation in polychaetous annelids also indicates plasticity of segment-generating mechanisms present in different annelid life histories (Seaver, Thamm, and Hill 2005). However, using the strict definition presented above, we believe that Myzostomida possess iterated organs, but are not truly segmented animals. Nevertheless,

this conclusion does not contradict our supposed annelid origin of myzostomids. Many annelids show extreme modifications of coelomic cavities, e.g., leeches (Brusca and Brusca 2003); some lack any trace of a coelom, e.g., the interstitial *Microphthalmus* (Smith, Lombardi, and Rieger 1986). Incomplete or reduced segmentation can be found in other annelid taxa like siboglinids or echiurids as well (Southward 1993; Halanych, Dahlgren, and McHugh 2002; Hessling and Westheide 2002).

Assuming that myzostomids are part of the annelid radiation, as supported by the molecular data presented here, we propose that iteration as observed in myzostomids represents a derived state from true segmentation as found in many annelids. Elucidation of annelid phylogeny and finding the sister taxon of Myzostomida will enable us to further evaluate this hypothesis.

Most myzostomids are hermaphrodites, and fertilization occurs through a spermatophore that penetrates the myzostomid body and reaches mature oocytes for internal fertilization (Eeckhaut and Jangoux 1991). Myzostomid spermatozoa are unique in that they bear an anterior flagellum with the centriolar structure at its apex and lack an accessory centriole (Afzelius 1983; Mattei and Marchand 1987). A similar spermatozoan is described for acanthocephalans (Mattei and Marchand 1987), but homology (as coded in the morphological character matrix of Zrzavy, Hypsa, and Tietz 2001) is not supported by our phylogenetic analyses.

Myzostomida and Lophotrochozoan Character Evolution

Previous investigations concluding that myzostomids are not closely related to annelids (Eeckhaut et al. 2000; Zrzavy, Hypsa, and Tietz 2001) suggested that all similarities present in these taxa are due to convergences or represent plesiomorphic traits. The question was raised if major morphological characters used for the classification of the Metazoa (e.g., segmentation, the presence/absence of a coelom, and the presence/absence of a specific larval stage) are not as conservative and “noise free” as is generally implied (Eeckhaut et al. 2000; Jenner 2001, 2004). We have shown that these conclusions can only partly be drawn from investigating Myzostomida, due to their phylogenetic affinity to annelids. Nevertheless, chitinous chaetae similar to that of Myzostomida and Annelida are also present in some Brachiopoda, Bryozoa, and Mollusca (reviewed in Hausen 2005), and a trochophore-like larvae is widespread within Lophotrochozoa (e.g., Rouse 1999; Nielsen 2001). We give further evidence that segmentation, as well as the possession, structure, and formation of coelomic cavities in annelids (and as such in Lophotrochozoa) is more plastic than traditionally assumed. Our results further highlight the need to assess such complex characters in the context of robust phylogenetic hypotheses, as advocated by Halanych (2004).

Supplementary Material

Supplementary figure are available at Molecular Biology and Evolution online (<http://www.mbe.oxfordjournals.org/>).

Acknowledgments

We thank G.W. Rouse (Scripps Institute, La Jolla, CA) for providing specimens of *Myzostoma seymourcollegiorum*. We thank J. Selbig and M. Ende for access to the Bioinformatics UNIX cluster of the University of Potsdam for phylogenetic inference and Anne Hoffer and Danielle Gleason (Colgate University) for technical assistance. C. Mayer (University of Bochum, Germany) and J.W. Wägele (A. Koenig Museum, Bonn, Germany) provided an unpublished version of the SAMS package.

We acknowledge financial support from the Deutsche Forschungsgemeinschaft in the priority program SPP 1174 “Deep Metazoan Phylogeny” to R.T. (TI 349/4–1) and L.P. (BA 1520/10–1) and by NSF EAR-0342392 “WormNet” to K.M.H. and D.M.H. I.E. and M.C.M. were supported through the National Fund for Scientific Research (FNRS–FRFC) Belgium.

Literature Cited

- Abascal F, Zardoya R, Posada D. 2005. ProtTest: selection of best-fit models of protein evolution. *Bioinformatics*. 21:2104–2105.
- Afzelius BA. 1983. The spermatozoon of *Myzostomum cirriferum* (Annelida, Myzostomida). *J. Ultrastruct Res.* 83:58–68.
- Bartolomaeus T, Purschke G, Hausen H. 2005. Polychaete phylogeny based on morphological data—a comparison of current attempts. *Hydrobiologia*. 535/536:341–356.
- Bartolomaeus T, Quast B. 2005. Structure and development of nephridia in Annelida and related taxa. *Hydrobiologia*. 535/536:139–165.
- Benham WB. 1896. Archiannelida, Polychaeta, Myzostomidaria. In: Farmer SF, Shipley AE, editors. *The Cambridge natural history*. London: Macmillan. p. 241–334.
- Bergsten J. 2005. A review of long-branch attraction. *Cladistics*. 21:163–193.
- Bleidorn C. 2005. Phylogenetic relationships and evolution of Orbiniidae (Annelida, Polychaeta) based on molecular data. *Zool J Linn Soc.* 144:59–73.
- Bleidorn C, Podsiadlowski L, Bartolomaeus T. 2006. The complete mitochondrial genome of the orbiniid polychaete *Orbinia latreillii* (Annelida, Orbiniidae)—a novel gene order for Annelida and implications for annelid phylogeny. *Gene*. 370:96–103.
- Bleidorn C, Vogt L, Bartolomaeus T. 2003. New insights into polychaete phylogeny (Annelida) inferred by 18S rDNA sequences. *Mol Phylogenet Evol.* 29:279–288.
- Boore JL. 1999. Animal mitochondrial genomes. *Nucleic Acids Res.* 27:1767–1780.
- Boore JL, Brown WM. 1998. Big trees from little genomes: mitochondrial gene order as a phylogenetic tool. *Curr Opin Gen Dev.* 8:668–674.
- Boore JL, Staton JL. 2002. The mitochondrial genome of the sipunculid *Phascolopsis gouldii* supports its association with Annelida rather than Mollusca. *Mol Biol Evol.* 19:127–137.
- Brusca RC, Brusca GJ. 2003. *Invertebrates*. Sunderland, MA: Sinauer Associates.
- Castresana J. 2000. Selection of conserved blocks from multiple alignments for their use in phylogenetic analysis. *Mol Biol Evol.* 17:540–552.
- Eeckhaut I. 1998. *Mycomyzostoma caldicola* gen. et sp. n., the first extant myzostomid infesting crinoid stalks, with a nomenclatural appendix by M.J. Grygier. *Spec Div.* 3:89–103.

- Eeckhaut I, Dochy B, Jangoux M. 1995. Feeding behaviour and functional morphology of the introvert and digestive system of *Myzostoma cirriferum* (Myzostomida). *Acta Zool.* 76: 307–315.
- Eeckhaut I, Fievez M, Müller MC. 2003. Larval development of *Myzostoma cirriferum* (Myzostomida). *J Morphol.* 258: 269–283.
- Eeckhaut I, Jangoux M. 1991. Fine structure of the spermaphore and intradermic penetration of sperm cells in *Myzostoma cirriferum* (Annelida, Myzostomida). *Zoomorphology.* 111:49–58.
- Eeckhaut I, Jangoux M. 1993. Integument and epidermal sensory structures of *Myzostoma cirriferum* (Myzostomida). *Zoomorphology.* 113:33–46.
- Eeckhaut I, Lanterbecq D. 2005. Myzostomida: A review of the phylogeny and ultrastructure. *Hydrobiologia.* 535/536: 253–275.
- Eeckhaut I, McHugh D, Mardulyn P, Tiedemann R, Monteyne D, Jangoux M, Milinkovitch MC. 2000. Myzostomida: a link between trochozoans and flatworms? *Proc R Soc Lond. B.* 267:1383–1392.
- Fedotov D. 1929. Beiträge zur Kenntnis der Morphologie der Myzostomiden. *Z. Morphol Ökol Tiere.* 15:156–191.
- Felsenstein J. 1978. Cases in which parsimony or compatibility methods will be positively misleading. *Syst Zool.* 27: 401–410.
- Fritzsche G, Schlegel M, Stadler PF. 2006. Alignments of mitochondrial genome arrangements: Applications to metazoan phylogeny. *J Theor Biol.* 240:511–520.
- Giribet G, Soerensen MV, Funch P, Kristensen RM, Sterrer W. 2004. Investigations into the phylogenetic position of Micrognathozoa using four molecular loci. *Cladistics.* 20:1–13.
- Graff L. 1877. Das Genus *Myzostoma* (F.S. Leuckhart). Leipzig: Wilhelm Engelmann.
- Grygier MJ. 2000. Myzostomida. In: Beesley PL, Ross GJB, Glasby CJ, editors. *Polychaetes and allies: the southern synthesis. Fauna of Australia, Vol 4A Polychaeta, Myzostomida, Pogonophora, Echiura, Sipuncula.* Melbourne: CSIRO Publishing. p. 297–330.
- Guindon S, Gascuel O. 2003. A simple, fast, and accurate algorithm to estimate large phylogenies by maximum likelihood. *Syst Biol.* 52:696–704.
- Halanych KM. 2004. The new view of animal phylogeny. *Ann Rev Ecol Evol Syst.* 35:229–256.
- Halanych KM, Dahlgren TG, McHugh D. 2002. Evidence that some lesser-known “phyla” are annelids. *Amer Zool.* 42: 678–684.
- Hall TA. 1999. BioEdit: a user-friendly biological sequence alignment editor and analysis program for Windows 95/98/NT. *Nucleic Acids Symp Ser.* 41:95–98.
- Haszprunar G. 1996. The Mollusca: coelomate turbellarians or mesenchymate annelids? In: Taylor JD, editor. *Origin and evolutionary radiation of the Mollusca.* Oxford: Oxford University Press. p. 3–28.
- Hausen H. 2005. Chaetae and chaetogenesis in polychaetes (Annelida). *Hydrobiologia.* 535/536:37–52.
- Hessling R, Westheide W. 2002. Are Echiura derived from a segmented ancestor? Immunohistochemical analysis of the nervous system in developmental stages of *Bonellia viridis*. *J Morphol.* 252:100–113.
- Huelsensbeck J. 1997. Is the Felsenstein zone a fly trap? *Syst Biol.* 46:69–74.
- Jägersten G. 1936. Zur Kenntnis der Parapodialborsten bei *Myzostomum*. *Zool Bidrag fran Uppsala.* 16:283–294.
- Jägersten G. 1940. Zur Kenntnis der Morphologie, Entwicklung und Taxonomie der Myzostomida. *Nova Acta Reg Soc Sci Ups.* 11:1–84.
- Jeanmougin F, Thompson JD, Gouy M, Higgins DG, Gibson TJ. 1998. Multiple sequence alignment with Clustal X. *Trends Biochem Sci.* 23:403–405.
- Jenner RA. 2001. Bilaterian phylogeny and uncritically recycling of morphological data sets. *Syst Biol.* 50:730–742.
- Jenner RA. 2003. Unleashing the force of cladistics? Metazoan phylogenetics and hypothesis testing. *Integr Comp Biol.* 43:207–218.
- Jenner RA. 2004. When molecules and morphology clash: reconciling conflicting phylogenies of the Metazoa by considering secondary character loss. *Evol Dev.* 6: 372–378.
- Jennings RM, Halanych KM. 2005. Mitochondrial genomes of *Clymenella torquata* (Maldanidae) and *Riftia pachyptila* (Siboglinidae). Evidence for conserved gene order in Annelida. *Mol Biol Evol.* 22:210–222.
- Jermiin LS, Ho SYW, Ababneh F, Robinson J, Larkum AWD. 2004. The biasing effect of compositional heterogeneity on phylogenetic estimates may be underestimated. *Syst Biol.* 53:638–643.
- Kass RE, Raftery AE. 1995. Bayes factors. *J Amer Stat Ass.* 90:773–795.
- Kato K. 1952. On the development of myzostome. *Sci Rep Saitama Univ. (B).* 1:1–16.
- Kennedy M, Holland BR, Gray RD, Spencer HG. 2005. Untangling long branches: Identifying conflicting phylogenetic signals using spectral analysis, neighbour-net, and consensus networks. *Syst Biol.* 54:620–633.
- Lanterbecq D, Bleidorn C, Michel S, Eeckhaut I. Locomotion and fine structure of parapodia in *Myzostoma cirriferum* (Myzostomida). *Zoomorphology submitted.*
- Lanterbecq D, Rouse GW, Milinkovitch MC, Eeckhaut I. 2006. Molecular phylogenetic analyses indicate multiple independent emergences of parasitism in Myzostomida (Protostomia). *Syst Biol.* 55:208–227.
- Lavrov DV, Lang BF. 2005. Poriferan mtDNA and animal phylogeny based on mitochondrial gene arrangements. *Syst Biol.* 54:651–659.
- Leuckart FS. 1827. Versuch einer naturgemässen Eintheilung der Helminthen. Heidelberg: Neue Akademische Buchhandlung von Karl Gross.
- Littlewood DTJ, Olson PD, Telford MJ, Herniou EA, Riutort M. 2001. Elongation Factor 1-alpha sequences alone do not assist in resolving the position of the Acoela within Metazoa. *Mol Biol Evol.* 18:437–442.
- Lowe TM, Eddy SR. 1997. tRNAscan-SE: a program for improved detection of transfer RNA genes in genomic sequence. *Nucleic Acids Res.* 25:955–964.
- Mayer C, Wägele JW. 2005. SAMS (Split analysis methods) Version 1.4 beta. Distributed by the authors.
- Mattei X, Marchand B. 1987. Les spermatozoïdes des Acanthocephales et des Myzostomides. Resemblances et conséquences phyletiques. Paris: C. R. Acad. Sci., Serie III, Sci. p. 525–529.
- McHugh D. 1997. Molecular evidence that echiurans and pogonophorans are derived annelids. *Proc Natl Acad Sci USA.* 94:8006–8009.
- McHugh D. 2005. Molecular systematics of polychaetes (Annelida). *Hydrobiologia.* 535/536:309–318.
- Müller MC, Westheide W. 2000. Structure of the nervous system of *Myzostoma cirriferum* (Annelida) as revealed by immunohistochemistry and cLSM analyses. *J Morphol.* 245:87–98.
- Nielsen C. 2001. *Animal evolution: Interrelationships of the living phyla.* New York: Oxford University Press.
- Nylander J, Ronquist F, Huelsenbeck J, Nieves-Aldrey J. 2004. Bayesian phylogenetic analysis of combined data. *Syst Biol.* 53:47–67.

- Passamanek Y, Halanych KM. 2006. Lophotrochozoan phylogeny assessed with LSU and SSU data: evidence of lophophorate polyphyly. *Mol Phylogenet Evol.* 40:20–28.
- Pietsch A, Wesheide W. 1987. Protonephridial organs in *Myzostoma cirriferum* (Myzostomida). *Acta Zool.* 68:195–203.
- Podsiadlowski L, Bartolomaeus T. 2005. Organization of the mitochondrial genome of mantis shrimp *Pseudosquilla ciliata* (Crustacea: Stomatopoda). *Mar Biotechnol.* 7:618–624.
- Posada D, Crandall KA. 1998. Modeltest: testing the model of DNA substitution. *Bioinformatics.* 14:817–818.
- Rambaut A, Grassly NC. 1997. Seq-Gen: an application for the Monte Carlo simulation of DNA sequence evolution along phylogenetic trees. *Comput Appl Biosci.* 13:235–238.
- Ronquist F, Huelsenbeck JP. 2003. MrBayes 3: Bayesian phylogenetic inference under mixed models. *Bioinformatics.* 19:1572–1574.
- Rouse GW. 1999. Trochophore concepts: ciliary bands and the evolution of larvae in spiralian Metazoa. *Biol J Linn Soc.* 66:411–464.
- Rouse GW, Fauchald K. 1997. Cladistics and polychaetes. *Zool Scr.* 26:139–204.
- Rouse GW, Grygier MJ. 2005. *Myzostoma seymourcollegiorum* n. sp. (Myzostomida) from southern Australia, with a description of its larval development. *Zootaxa.* 1010:53–64.
- Rouse GW, Pleijel F. 2001. *Polychaetes*. Oxford: Oxford University Press.
- Ruiz-Trillo I, Paps J, Loukota M, Ribera C, Jondelius U, Baguna J, Riutort M. 2002. A phylogenetic analysis of myosin heavy chain type II sequences corroborates that Acoela and Nemertodermatida are basal bilaterians. *Proc Nat Acad Sci USA.* 99:11246–11251.
- Schmidt HA, Strimmer K, Vingron M, von Haeseler A. 2002. TREE-PUZZLE: maximum likelihood phylogenetic analysis using quartets and parallel computing. *Bioinformatics.* 18:502–504.
- Scholtz G. 2002. The Articulata hypothesis—or what is a segment? *Org Divers Evol.* 2:197–215.
- Seaver EC. 2003. Segmentation: mono- or polyphyletic? *Int J Dev Biol.* 47:583–595.
- Seaver EC, Thamm K, Hill SD. 2005. Growth patterns during segmentation in the two polychaete annelids, *Capitella* sp. I and *Hydroides elegans*: comparisons at distinct life history stages. *Evol Dev.* 7:312–326.
- Semper C. 1858. Zur Anatomie und Entwicklungsgeschichte der Gattung *Myzostoma* Leuckhart. *Z Wiss Zool.* 9:48–65.
- Simon C, Buckley TR, Frati F, Stewart JB, Beckenbach AT. 2006. Incorporating molecular evolution into phylogenetic analysis, and a new compilation of conserved polymerase chain reaction primers for animal mitochondrial DNA. *Ann Rev Ecol Evol Syst.* 37:545–579.
- Smith JPS, Lombardi J, Rieger RM. 1986. Ultrastructure of the body cavity lining in a secondary acoelomate, *Microphthalmus cf listensis* Westheide (Polychaeta, Hesionidae). *J Morph.* 188p. 257–271.
- Southward EC. 1993. Pogonophora. In: Harrison FW, Rice ME, editors. *Microscopic anatomy of invertebrates*, vol. 12. Onychophora, Chilopoda and lesser Protostomata. New York: Wiley-Liss. p. 327–369.
- Steel MA. 1994. Recovering a tree from the leaf colorations it generates under a Markov model. *Appl Math Lett.* 7:19–24.
- Swofford DL. 2002. PAUP*: Phylogenetic Analysis Using Parsimony (*and other methods). Sunderland, MA: Sinauer Associates.
- Tautz D. 2004. Segmentation. *Dev Cell.* 7:301–312.
- Thompson JD, Higgins DG, Gibson TJ. 1994. CLUSTAL W: improving the sensitivity of progressive multiple sequence alignment through sequence weighting, position specific gap penalties and weight matrix choice. *Nucleic Acids Res.* 22:4673–4680.
- Vallés Y, Boore JL. 2006. Lophotrochozoan mitochondrial genomes. *Integr Comp Biol.* 46:544–557.
- Wägele JW, Rödding F. 1998. A priori estimation of phylogenetic information conserved in aligned sequences. *Mol Phylogenet Evol.* 9:358–365.
- Willmer P. 1990. *Invertebrate relationships. Patterns in animal evolution*. New York: Cambridge University Press.
- Wyman SK, Jansen RK, Boore JL. 2004. Automatic annotation of organellar genomes with DOGMA. *Bioinformatics.* 20:3252–3255.
- Xia X, Xie Z. 2001. DAMBE: Data analysis in molecular biology and evolution. *J. Hered.* 92:371–373.
- Zrzavy J, Hypsa V, Tietz D. 2001. Myzostomida are not annelids: molecular and morphological support for a clade of animals with anterior sperm flagella. *Cladistics.* 17: 1–29.

Billie Swalla, Associate Editor

Accepted April 25, 2007